



Terahertz antenna with tunable filtering characteristics

Durgesh Kumar¹ · Aditi Sharma¹ · Aarushi Arora¹ · Pushpa Giri¹ · Gaurav Varshney¹ 

Received: 18 May 2022 / Accepted: 8 October 2022 / Published online: 22 October 2022

© The Author(s), under exclusive licence to Springer Science+Business Media, LLC, part of Springer Nature 2022

Abstract

A terahertz (THz) antenna with metallic radiator is designed to provide the monopole like radiation characteristics and ultra-wideband (UWB) response. An antenna with metallic radiator is designed to operate in the frequency range 1.78–5.48 THz. A graphene disc is applied beneath the substrate of antenna opposite to the metal radiator. The confinement of electric field in the area of graphene disc can be varied using the chemical potential of graphene (μ_c). This leads to alter the surface plasmon resonance and provides the sharp filtering characteristics in UWB response which can be tuned by altering the chemical potential of graphene. This antenna operates in the frequency range 1.78–5.39 THz for $\mu_c=0$ eV without filtering response. For $\mu_c=0.8$ eV, this antenna provides the operation over 1.67–5.64 THz with the filtered band of frequency 3.2–3.97 THz. The antenna operation is verified with the analysis using electrical circuit model.

Keywords Antenna · Band notch · Graphene · Tunable · THz · UWB

1 Introduction

Terahertz (THz) frequency spectrum is being investigated for the implementations of future wireless systems due to its feature that it has the capability of providing wide bandwidth (Akyildiz et al. 2014). The wide bandwidth offered by THz spectrum can provide the higher data transfer rate which is the main requirement of future wireless technology (He et al. 2020; Burford and El-Shenawee 2017). It can offer the properties of radiation like microwave and infrared frequency spectrum (Varshney and Giri 2021; Khan et al. 2021). The application sectors of THz spectrum are being expected as medical, defense and communication in imaging and sensing (Mumtaz et al. 2017; Tekbıyık et al. 2019; Son et al. 2019; Forsythe et al. 1991; Roggo et al. 2005; Zhang et al. 2020). Also, THz spectrum can offer its significant usability in food technology for the detection of viruses and toxicity (Afsah-Hejri et al. 2019). The advancements in wireless systems require antennas with reconfigurability in radiation pattern and frequency response (Varshney 2020a; Varshney et al. 2019a). A recent article had briefed about the latest developments in THz antennas

✉ Gaurav Varshney
gauravnitd@outlook.com

¹ Department of Electronics and Communication Engineering, National Institute of Technology Patna, Patna 800005, India

that these can be implemented with the usage of metal, dielectric and graphene material-based radiators (Varshney 2020b). The usage of dielectric radiator-based antennas are efficient but their operation is restricted due to they offer large height (Gupta et al. 2021; Varshney and Sahana 2021; Sahana and Varshney, 2022; Gotra et al. 2020). They may not be compatible with small-scale systems and they do not offer the inherent tunability. Another category of THz antennas is based on the graphene material which can provide the tunable antenna response (Varshney 2020a; Farman et al. 2021; Varshney et al. 2020). The ability of graphene material in offering the tunable electronic properties can provide the tunable antenna response (Cao et al. 2016; Hanson 2008a; Chen et al. 2013; Wang et al. 2015; Correas-Serrano et al. 2015; Naghdehforushha and Moradi 2017). The limitation of antennas with graphene-based resonating unit is that they are a poor radiator (Hosseininejad et al. 2018; Abadal et al. 2013, 2019; Kiani et al. 2020; Naghdehforushha and Moradi 2019). Third category is about the utilization of metal-based radiators in THz antennas (Naik et al. 2021; Murali et al. 2021; Singhal 2019a; Keshwala et al. 2020). The microstrip technology has been serving the wireless technology around for last more than four decades specially at microwave spectrum (Losada et al. 1999; Richards et al. 1981; Lee and Tong 2012). The microstrip-based antennas can offer efficient radiation performance along with the small size which can overwhelm the future THz technology as well (Lee and Tong 2012; Michalski and Zheng 1992; Sharma 2020; Das and Varshney 2022).

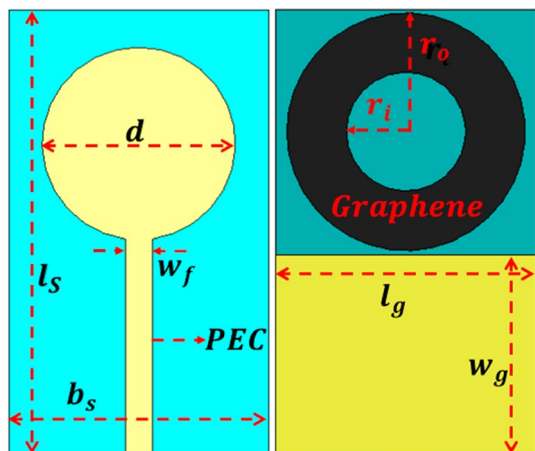
Furthermore, the focus of researchers in current time is to implement the THz antenna with ultra-wideband (UWB) response (Keshwala et al. 2021; Varshney 2020c; Sharma et al. 2020, 2022; Singhal 2021a, 2021b). Here, the term UWB is being referred for defining the feature of any antenna providing the bandwidth more than few giga hertz (GHz). The usage of UWB systems in communication technology can allow the long-distance transmission with short duration pulses. This feature of UWB systems can be suitable in radar systems. The recent developments in THz radar systems can seek the advanced antennas with UWB response (Forsythe et al. 1991). THz UWB antennas can have advanced features if they are able to offer the inbuilt filtering capability (Srivastava et al. 2021). The inbuilt filtering characteristics in antenna response can prevent the usage of external filters (Srivastava et al. 2021). There are a number of techniques available in microwave antennas which suggest the technique of generation of tunable stop band in antenna response like usage of switches, diodes and relays (Srivastava et al. 2021). The small dimensions of THz antenna do not allow to use these switching devices in the circuit. The recent development in THz UWB antennas shows that graphene strips can provide the band notch characteristics in UWB response (Sharma et al. 2020). The alteration in electronic properties of graphene material can offer the tunability in achieved band notch over frequency. However, this is still a challenging task.

Based on the above discussions, current research issue can be summarized as; implementing the THz antenna with tunable filtering response which has been followed here in this article and a simple solution is reported. A graphene disc is placed beneath the substrate in opposite to the radiating patch which confines the localized surface plasmons and thus anti-resonance is created in the specific frequency range for achieving the filtering characteristics. The alteration in electrical properties of graphene material can provide the tunability in the created notched frequency band. The proposed research work reports a simplest technique for obtaining the filtering characteristics in UWB response of THz antenna. The simple antenna geometry can allow it to be used in the implementation of antenna arrays with UWB response and engraved filtering characteristics. Also, this geometry can allow the implementation of multipoint antennas with UWB response along with the filtering characteristics.

2 Antenna design and evolution

The final antenna structure is shown in Fig. 1. The antenna structure contains the simple metal-based radiator of diameter d connected to a microstrip feedline of width w_f at one side of the substrate of height $h_s = 1.6\mu\text{m}$ and half ground plane structure at its another side. The substrate of polyimide with the relative permittivity $\epsilon_s = 3.5$ having dimensions $l_s \times b_s$ is used for implementing the antenna structure. Fabrication of antenna can be done with the substrate having metal coating at its both sides which can be grown using sputtering technique. The metallic coating can be patterned to form the shape of radiator and ground plane using electronic beam lithography (Suñé 2008). The antenna contains the ground plane of size $l_g \times w_g$ which covers the half-size of the substrate. The structure of this antenna is shown in Fig. 2a and mentioned by the name as antenna-1 and it provides the UWB response as plotted in Fig. 2b. The dimensions of this antenna have been selected using the traditional approach used for designing the microstrip antennas (James and Hall 1990). This antenna structure is then modified with the engraving of graphene disc of outer and inner radius as r_o and r_i , respectively beneath to the substrate in opposite to the circular metallic radiator. This antenna structure is mentioned by antenna-2 with its top and bottom view in Fig. 2a. The application of graphene disc with chemical potential $\mu_c = 0\text{eV}$, relaxation time $\tau = 1\text{ps}$ at temperature $T = 300\text{K}$ provides the antenna response as similar as antenna-1. Antenna starts providing the band notch characteristics with the application of graphene with $\mu_c = 0.8\text{eV}$. The antenna structure is implemented using CST microwave studio. The dimensions of antenna are mentioned in Table 1. Figure 2c shows the impedance plot of antenna-2 with μ_c as 0 and 0.8eV. The impedance plot shows the generation of multiple resonances in the antenna structure for providing the UWB response. Also, the mode pattern is drastically disturbed in the region of frequency where band notch is achieved. It can be seen that antenna with $\mu_c = 0\text{eV}$ operates with three resonances m_1 , m_2 and m_3 . For $\mu_c = 0.8\text{eV}$, two more resonances are also generated m_{g_1} and m_{g_2} at the center frequency and merged with the resonance of circular patch. Varying the chemical potential of graphene can tune the resistivity and hence the impedance matching at the generated surface plasmon resonance due to the addition of the graphene ring. Thus, the impedance matching at the frequency of the generated surface plasmon resonance can be tuned to generate the band notch. A discussion about the surface conductivity and its electrical

Fig. 1 Top (left) and bottom (right) view of antenna structure



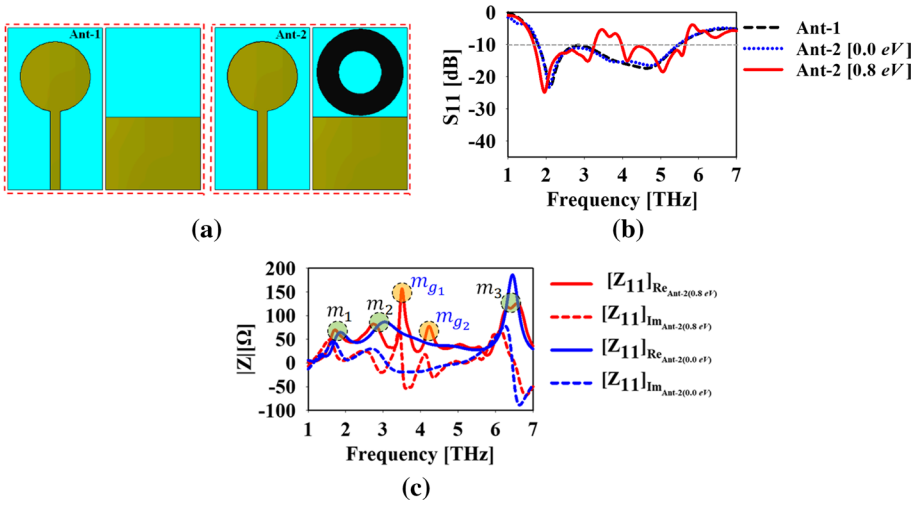


Fig. 2 **a** Antenna evolution containing the structure of antenna-1 and 2, their **b** reflection coefficient and **c** impedance plot

Table 1 The dimensions of antenna structure (all dimensions in μm)

Parameters	l_s	b_s	w_f	l_g	w_g	d	r_o	r_i
Dimensions	60	35	3.60	35	27	26	16	08

Table 2 The performance of antenna-1 and 2

Antenna	Operating frequency (THz)	Filtered frequency band (THz)
Antenna-1	1.78 – 5.48	–
Antenna-2 ($\mu_c = 0\text{eV}$)	1.78 – 5.39	–
Antenna-2 ($\mu_c = 0.8\text{eV}$)	1.67 – 5.64	3.2 – 3.97

properties is reported in the next section of this manuscript. The performance of antenna-1 and 2 is reported in Table 2. The antenna operation is verified with the electrical equivalent circuit model shown in Fig. 3. The electrical circuit model is prepared with five parallel RLC circuits for representing it with $\mu_c = 0.8\text{eV}$. The resistance of the two tank circuits corresponding to m_{g1} and m_{g2} is represented by the variable resistance due to the fact that surface conductivity and hence the resistivity of graphene can be set using an external electrostatic voltage. Thus, the impedance matching of these two central tank circuits can be set accordingly and hence the antenna operation without and with the band notch can be verified. All the circuit parameters have been calculated using circuit theory approach as already reported in the case of a graphene antenna and mentioned in Table 3 (Varshney 2020a).

Figure 4 shows the effect of varying the physical parameter of antenna, r_o and r_i . The best values of these parameters by maintaining the appropriate impedance matching in the passband and with the highest value of reflection coefficient is 16 and 8 μm , respectively.

Fig. 3 **a** Equivalent electrical circuit model and its S_{11} parameter response with $\mu_c = \mathbf{b}$ 0 and **c** 0.8eV

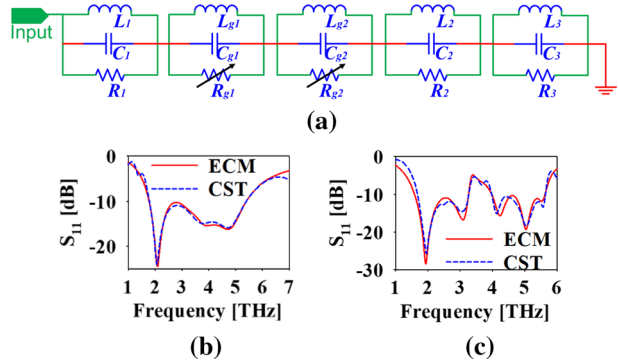


Table 3 The circuit parameters of equivalent circuit model

Para	Value	Para	Value	Para	Value	Para	Value	Para	Value
R_1	50.46Ω	R_2	59.04Ω	R_3	59.76Ω	R_{g1}	134.6Ω	R_{g2}	26.64Ω
L_1	0.236pH	L_2	0.0.117pH	L_3	0.174pH	L_{g1}	0.171pH	L_{g2}	0.143pH
C_1	0.0.00334pF	C_2	0.0.0066pF	C_3	0.0053pF	C_{g1}	0.01302pF	C_{g2}	0.01016pF

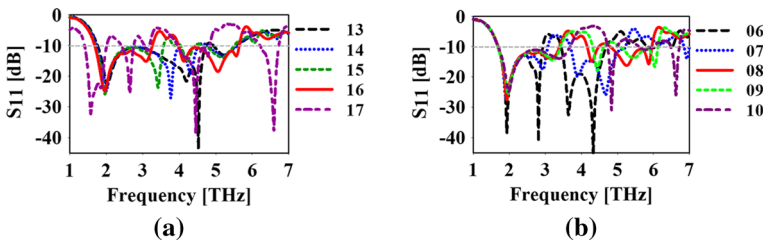


Fig. 4 S-parameter response with variable **a** r_o **b** r_i with $\mu_c = 0.8eV$

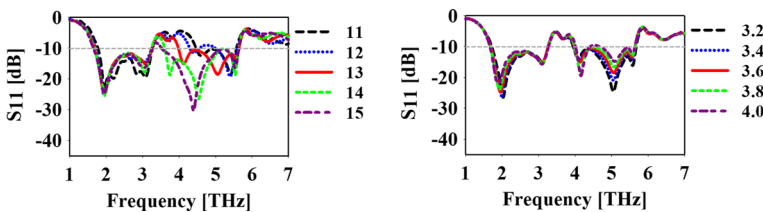


Fig. 5 S-parameter response with variable **a** $d/2$ and **b** w_f

The upper passband can be contracted to the small impedance bandwidth for lower values of r_i . In fact, there are certain values of r_o with which antenna does not provide the filtering action. Figure 5 shows the antenna response with variable radius of the radiating patch and width of the feedline. The radius of radiating patch can be set to provide the desired bandwidth of the created notched band. Also, the impedance matching is only affected by the width of the feedline, as expected.

3 Tunability in notch band

The alteration of Fermi energy using the applied electrostatic voltage on it can provide the tunability in the antenna response (Gale et al. 2012; Taghioskoui 2009; Warner et al. 2013). The surface conductivity of graphene can be represented in two parts; intraband and interband (Hanson 2008b). The intraband part of the surface conductivity is greatly affected in the lower THz frequency ranges with insignificant alteration in its interband part. The surface conductivity of graphene can be represented using the Drude’s model and Kubo’s formalism. The dependency of intraband surface conductivity of graphene on μ_c and applied electrostatic voltage is given in Eq. (1) and (2), (Hanson 2008b; Wang et al. 2019; Varshney et al. 2018a, 2019b).

$$\sigma_{intra}(\omega, \mu_c, \Gamma, T) = -j \frac{e^2 K_B T}{\pi \hbar^2 (\omega - j2\Gamma)} \left(\frac{\mu_c}{K_B T} + 2 \ln \left(e^{-\frac{\mu_c}{K_B T}} + 1 \right) \right) \tag{1}$$

$$V_g = \frac{e \mu_c^2 h_s}{\pi \hbar^2 v_f^2 \epsilon_o \epsilon_r} \tag{2}$$

Here, the terms $e, T, K_B, \mu_c, \Gamma, v_f, \epsilon_o, \epsilon_r$ respectively, stand for the electron’s charge of electron, temperature, the Boltzmann constant, the chemical potential of graphene, scattering rate, the reduced Plank’s constant, the Fermi velocity of the charge in the graphene layer, the free space permittivity, and the relative permittivity of the spacer between the graphene sheet To adjust the electrical properties of graphene, a DC voltage called V_g is provided to the graphene loop which is inserted to back side of substrate. The response of the proposed antenna with the variation in chemical potential of graphene is reported in Fig. 6. The S_{11} parameter response shows that the created band notch in the antenna response can be tuned over the frequency by keeping the lower 10 dB cut-off points approximately fixed. Thus, the proposed antenna can provide the response with the tunable band notch characteristics.

The operation of creation of the stop band can be analyzed using the electric field distribution on the antenna structure as illustrated in Fig. 7. The magnitude of the electric field is drawn at the frequency of passband and stopband without and with the graphene applied in the antenna structure. The difference in the electric field distribution is clear specifically at the frequency of the band notch. It can be seen that there is no field confinement at the bottom of the substrate at frequency 3.14 THz which is the band notch frequency. The application of graphene disc can provide the heavy confinement of electric field on it which results in mitigating the radiating resonant modes at this frequency.

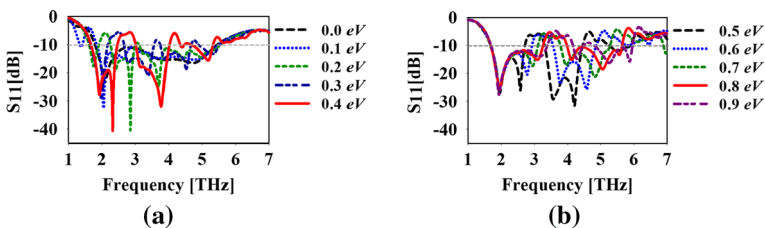
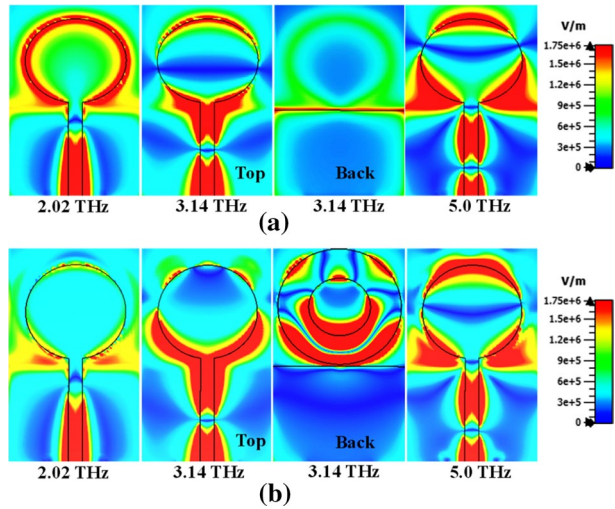


Fig. 6 a and b S-parameter response with variable μ_c

Fig. 7 Electric field distribution on antenna **a** 1 (first row) **b** 2 at $\mu_c = 0.8eV$ (second row)



This may be due to the fact that the generated surface plasmon resonance can be in opposite phase to the resonant modes on the antenna radiator at this frequency which leads to provide the filtering action. The combined effect of graphene and metal radiator can be understood from the impedance plot which shows the large imaginary part of the reactive impedance at the frequency of filtered band. This confirms that the resonance of adverse phase has been generated in the filtered frequency band due to the placement of graphene in antenna.

The far-field performance of antenna is studied by drawing the 3D gain pattern as illustrated in Fig. 8. The gain pattern has been drawn in the case of antenna without and with graphene. The antenna offers the radiation pattern like a monopole antenna with the high value of gain in the passband. Also, antenna provides inferior radiation behavior at band notch frequency confirming the sharp filtering response is being obtained from the antenna.

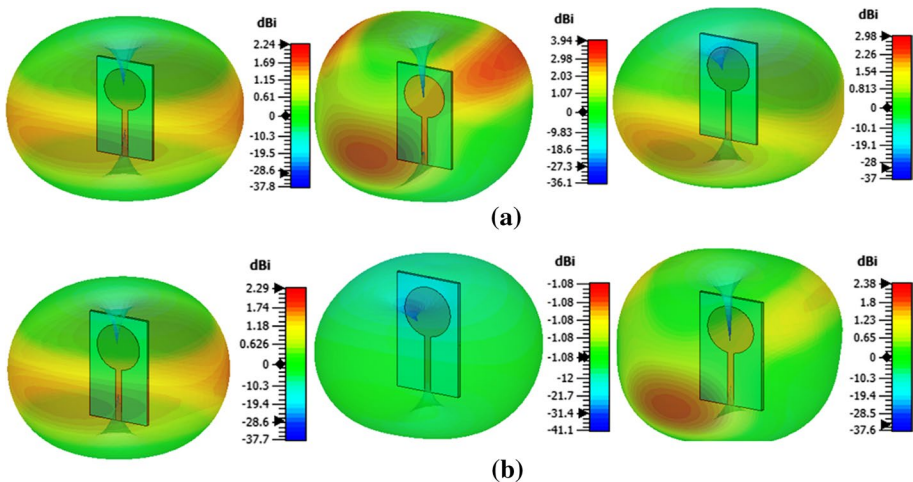


Fig. 8 3D gain pattern of antenna **a** 1 **b** 2 at 2.02 (left), 3.45 (middle) and 5 THz (right) with $\mu_c = 0.8eV$

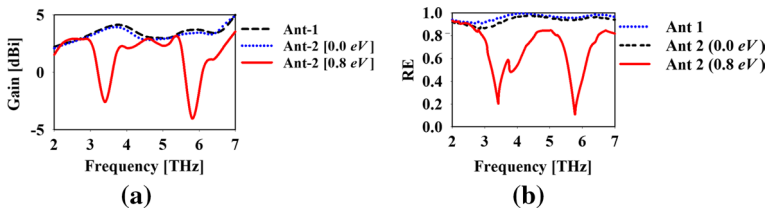


Fig. 9 **a** Gain and **b** radiation efficiency of all the antennas

Moreover, the plot of gain and radiation efficiency is drawn in Fig. 9. The comparison of gain plot of antenna-1 and 2 (with different values of μ_c) is reported in Fig. 9a. This clearly represents that antenna-2 with $\mu_c = 0.8$ eV follows the pattern of gain as antenna-1 in the passband but its gain is drastically reduced in the filtered bands, as expected. The sharp roll-off rate of decay of gain in the stopband makes the proposed technique proficient if THz antenna is required to be implemented with tunable filtering response. The antenna without graphene provides the radiation efficiency around more than 90% in the passband and similar is maintained in the case of when graphene disc is applied with $\mu_c = 0$ eV. Setting the value of μ_c as 0.8 eV provides the band notch operation and hence the low value of radiation efficiency is obtained in the frequency region of the created band notch. Also, the application of graphene reduces radiation efficiency of antenna to level of 80% in the case the graphene disc is applied with $\mu_c = 0.8$ eV. The reduction in the radiation efficiency is due to the absorbing nature of the graphene material.

A comparison of the proposed antenna with others available THz UWB antennas is reported in Table 4. This shows that the proposed antenna can provide a way of implementing the THz UWB antenna with the tunable filtering response. Most of other antennas are not providing the filtering response (Poorgholam-Khanjari et al. 2020; Varshney et al. 2018b; Varshney 2020d). In fact, the antenna which is providing the tunable response is not efficient (Varshney et al. 2018b). The antenna which is providing the tunable filtering response is also less efficient (Sharma et al. 2020). Thus, one can conclude the proposed antenna as simple and suitable for THz communication where tunable filtering response is required.

4 Conclusion

A THz antenna with metallic radiator has been designed to provide the monopole like radiation characteristics and UWB response. A graphene disc has been applied beneath the substrate of antenna opposite to the metal radiator. The confinement of electric field in the area covered by the graphene disc has been varied using the chemical potential of graphene. This leads to generate the surface plasmons which suppressed the resonating modes of antenna at certain frequencies for specific value of chemical potential of graphene. Thus, band notch characteristics in UWB response has been obtained. The tunability in the created band notch has been obtained with the variation in the chemical potential of graphene. The antenna can be utilized in THz communication systems which require to guard the specific frequency ranges by preventing the external filters.

Table 4 Comparison with other UWB antennas

Ref	Antenna radiator	Operating frequency [THz]	Notched band	Impedance bandwidth (%)	Gain (dBi)	Radiation efficiency (%)	Tunability
Sharma et al. (2020)	Metal Graphene nanoribbons	4.76–19	Yes	119.86	≥ 6.4	≥ 80	Yes
Poorgholam-Khanjari et al. (2020)	Metallic Yagi-Uda type	1.84–2.42	No	27	3.9	100	No
Varshney et al. (2018b)	Graphene patch	0.8–3.34	No	109.25	–	–	Yes
Varshney (2020d)	Graphite Disk Resonator	5–15	No	100	–	–	No
Singhal (2019b)	Metallic patch	0.46–5.46	No	168.92	≥ 9.5	≥ 96	No
This work	Metal Patch	1.78–5.48	No	118.6	4.13	≥ 94	No
	Metal/graphene hybrid patch	1.78–5.39	No	100.6	3.94	≥ 93	Yes
		$(\mu_c = 0eV)$					
		1.67–5.64	Yes	108.6	2.93	≥ 85	Yes
		$(\mu_c = 0.8eV)$					

Bold represents the parameters of this research work

Author contributions DK: has developed and implemented the idea of the reported research work, AS and AA: have implemented the research work and prepared the manuscript, PG has supervised the research work, GV: has developed the idea and supervised the research work. All the authors discussed and prepared the manuscript.

Funding There is no funding support to this research work.

Data availability No data is associated with this research work.

Declarations

Conflict of interest There is no competing interests among the authors.

Ethical Approval Not applicable.

References

- Abadal, S., Alarcón, E., Cabellos-Aparicio, A., Lemme, M., Nemirowsky, M.: Graphene-enabled wireless communication for massive multicore architectures. *IEEE Commun. Mag.* **51**(11), 137–143 (2013). <https://doi.org/10.1109/MCOM.2013.6658665>
- Abadal, S., et al.: Graphene-based antenna design for communications in the terahertz band. *Nanoscale networking and communications handbook*, pp. 25–45 (2019)
- Afsah-Hejri, L., Hajeb, P., Ara, P., Ehsani, R.J.: A comprehensive review on food applications of terahertz spectroscopy and imaging. *Compr. Rev. Food Sci. Food Saf.* **18**(5), 1563–1621 (2019). <https://doi.org/10.1111/1541-4337.12490>
- Akyildiz, I.F., Jornet, J.M., Han, C.: Terahertz band: next frontier for wireless communications. *Phys. Commun.* **12**, 16–32 (2014). <https://doi.org/10.1016/j.phycom.2014.01.006>
- Burford, N.M., El-Shenawee, M.O.: Review of terahertz photoconductive antenna technology. *Opt. Eng.* **56**(1), 010901 (2017). <https://doi.org/10.1117/1.OE.56.1.010901>
- Cao, Y.S., Jiang, L.J., Ruehli, A.E.: An equivalent circuit model for graphene-based terahertz antenna using the PEEC method. *IEEE Trans. Antennas Propag.* **64**(4), 1385–1393 (2016). <https://doi.org/10.1109/TAP.2016.2521881>
- Chen, P.Y., Argyropoulos, C., Alu, A.: Terahertz antenna phase shifters using integrally-gated graphene transmission-lines. *IEEE Trans. Antennas Propag.* **61**(4), 1528–1537 (2013). <https://doi.org/10.1109/TAP.2012.2220327>
- Correas-Serrano, D., Gomez-Diaz, J.S., Alu, A., Alvarez-Melcon, A.: Electrically and magnetically biased graphene-based cylindrical waveguides: analysis and applications as reconfigurable antennas. *IEEE Trans. Terahertz Sci. Technol.* **5**(6), 951–960 (2015). <https://doi.org/10.1109/TTHZ.2015.2472985>
- Das, P., Varshney, G.: Gain enhancement of dual-band terahertz antenna using reflection-based frequency selective surfaces. *Opt. Quantum Electron.* **54**(3), 1–23 (2022). <https://doi.org/10.1007/s11082-022-03548-4>
- Farman Ali, M., Bhattacharya, R., Varshney, G.: Graphene-based tunable terahertz self-diplexing/MIMO STAR antenna with pattern diversity. *Nano Commun. Netw.* **30**, 100378 (2021)
- Forsythe, R.E., Bohlander, R.A., Butterworth, J.C.: An experimental 225 GHz pulsed coherent radar. *IEEE Trans. Microw. Theory Tech.* **39**(3), 555–562 (1991). <https://doi.org/10.1109/22.75300>
- Gale, J.D., et al.: The rise of graphene. *Rev. Mod. Phys.* **58**(1), 710–734 (2012). <https://doi.org/10.1016/j.jmps.2010.02.008>
- Gotra, S., Pandey, V.S., Yaduvanshi, R.S.: A wideband graphene coated dielectric resonator antenna with circular polarization generation technique for THz applications. *Superlattices Microstruct.* **150**, 106754 (2021). <https://doi.org/10.1016/j.spmi.2020.106754>
- Gupta, R., Varshney, G., Yaduvanshi, R.S.: Tunable terahertz circularly polarized dielectric resonator antenna. *Optik* **239**, 166800 (2021). <https://doi.org/10.1016/j.ijleo.2021.166800>
- Hanson, G.W.: Dyadic green's functions for an anisotropic, non-local model of biased graphene. *IEEE Trans. Antennas Propag.* **56**(3), 747–757 (2008a). <https://doi.org/10.1109/TAP.2008.917005>
- Hanson, G.W.: Dyadic green's functions for an anisotropic, non-local model of biased graphene. *IEEE Trans. Antennas Propag.* **56**(3), 747–757 (2008b). <https://doi.org/10.1109/TAP.2008.917005>

- He, Y., Chen, Y., Zhang, L., Wong, S.W., Chen, Z.N.: An overview of terahertz antennas. *China Commun.* **17**(7), 124–165 (2020). <https://doi.org/10.23919/J.CC.2020.07.011>
- Hosseininejad, S.E., et al.: Reconfigurable THz plasmonic antenna based on few-layer graphene with high radiation efficiency. *Nanomaterials* **8**(8), 1–7 (2018). <https://doi.org/10.3390/nano8080577>
- James, J.R., Hall, P.S.: Handbook of microstrip antennas, 36(9), p. 354 (1990)
- Keshwala, U., Ray, K., Rawat, S.: Ultra-wideband mushroom shaped half-sinusoidal antenna for THz applications. *Optik* **228**, 166156 (2021). <https://doi.org/10.1016/j.jpleo.2020.166156>
- Khan, M.S., Varshney, G., Giri, P.: Altering the multimodal resonance in ultrathin silicon ring for tunable THz biosensing. *IEEE Trans. Nanobioscience* **20**(4), 488–496 (2021). <https://doi.org/10.1109/TNB.2021.3105561>
- Kiani, N., TavakkolHamedani, F., Rezaei, P., JafariChashmi, M., Danaie, M.: “Polarization controlling approach in reconfigurable microstrip graphene-based antenna. *Optik* **203**, 163942 (2020)
- Lee, K.F., Tong, K.F.: Microstrip patch antennas basic characteristics and some recent advances. *Proc. IEEE* **100**(7), 2169–2180 (2012). <https://doi.org/10.1109/JPROC.2012.2183829>
- Losada, V., Boix, R.R., Horno, M.: Resonant modes of circular microstrip patches in multilayered substrates. *IEEE Trans. Microw. Theory Tech.* **47**(4), 488–498 (1999). <https://doi.org/10.1109/22.754883>
- Michalski, K.A., Zheng, D.: Analysis of microstrip resonators of arbitrary shape. *IEEE Trans. Microw. Theory Tech.* **40**(1), 112–119 (1992). <https://doi.org/10.1109/22.108330>
- Mumtaz, S., Jornet, J.M., Aulin, J., Gerstaecker, W.H., Dong, X., Ai, B.: Terahertz communication for vehicular networks. *IEEE Trans. Veh. Technol.* **66**(7), 5617–5625 (2017). <https://doi.org/10.1109/TVT.2017.2712878>
- Murali, C., Sudipta, K., Anveshkumar, D., Soufian, N., Boddapati, L., Phani, T.: A micro-sized rhombus-shaped THz antenna for high-speed short-range wireless communication applications. *Plasmonics* **16**, 2167–2177 (2021). <https://doi.org/10.1007/s11468-021-01472-z>
- Naghdehforushha, S.A., Moradi, G.: Design of plasmonic rectangular ribbon antenna based on graphene for terahertz band communication. *IET Microw. Antennas Propag.* **12**(5), 804–807 (2017). <https://doi.org/10.1049/iet-map.2017.0678>
- Naghdehforushha, S.A., Moradi, G.: An improved method to null-fill H-plane radiation pattern of graphene patch THz antenna utilizing branch feeding microstrip line. *Optik* **181**, 21–27 (2019). <https://doi.org/10.1016/j.jpleo.2018.11.155>
- Naik, K.K., Suman, M., Rao, E.K.: Design of complementary split ring resonators on elliptical patch antenna with enhanced gain for terahertz applications. *Optik* **243**, 167434 (2021). <https://doi.org/10.1016/j.jpleo.2021.167434>
- Poorgholam-Khanjari, S., Zarrabi, F.B., Jarchi, S.: Compact and wide-band Quasi Yagi-Uda antenna based on periodic grating ground and coupling method in terahertz regime. *Optik* **203**, 163990 (2020). <https://doi.org/10.1016/j.jpleo.2019.163990>
- Richards, W.F., Lo, Y.T., Harrison, D.D.: An improved theory for microstrip antennas and applications. *IEEE Trans. Antennas Propag.* **29**(1), 38–46 (1981). <https://doi.org/10.1109/TAP.1981.1142524>
- Roggo, Y., Jent, N., Edmond, A., Chalus, P., Ulmschneider, M.: Characterizing process effects on pharmaceutical solid forms using near-infrared spectroscopy and infrared imaging. *Eur. J. Pharm. Biopharm.* **61**(1–2), 100–110 (2005). <https://doi.org/10.1016/j.ejpb.2005.04.005>
- Sahana, B.C., Varshney, G.: Tunable terahertz dual-band circularly polarized dielectric resonator antenna. *Optik* **253**, 168578 (2022). <https://doi.org/10.1016/j.jpleo.2022.168578>
- Sharma, T.: Obtaining the tunable band-notch in ultrawideband THz antenna using graphene nanoribbons. *Opt. Eng.* **59**(4), 1 (2020). <https://doi.org/10.1117/1.OE.59.4.047103>
- Sharma, T., Varshney, G., Vashishath, R.S.Y.M.: Obtaining the tunable band-notch in ultrawideband THz antenna using graphene nanoribbons. *Opt. Eng.* **59**(4), 1 (2020). <https://doi.org/10.1117/1.OE.59.4.047103>
- Sharma, T., Varshney, G., Yaduvanshi, R.S., Vashishath, M.: Modified Koch borderline monopole antenna for THz regime. *Opt. Quantum Electron.* **54**(5), 1–16 (2022). <https://doi.org/10.1007/s11082-022-03687-8>
- Singhal, S.: Asymmetrically fed trapezoidal superwideband pattern diversity antenna. *Sci. Total Environ.* **231**, 135907 (2019). <https://doi.org/10.1016/j.jpleo.2021.166358>
- Singhal, S.: Ultrawideband elliptical microstrip antenna for terahertz applications. *Microw. Opt. Technol. Lett.* **61**(10), 2366–2373 (2019b). <https://doi.org/10.1002/mop.31910>
- Singhal, S.: CPW fed jasmine shaped superwideband terahertz antenna for pattern diversity applications. *Opt. Int. J. Light Electron Opt.* **231**, 166356 (2021). <https://doi.org/10.1016/j.jpleo.2021.166356>
- Singhal, S.: CPW fed circular sierpinski terahertz antenna for superwideband pattern diversity applications. *Optik* **243**, 105514 (2021). <https://doi.org/10.1016/j.jpleo.2021.167430>

- Son, J.H., Oh, S.J., Cheon, H.: Potential clinical applications of terahertz radiation. *J. Appl. Phys.* **125**(19), 190901 (2019). <https://doi.org/10.1063/1.5080205>
- Srivastava, K., Varshney, G., Singh, R.: Compact ultra-wideband monopole antenna with tunable notch bandwidth/frequency ratio. *Frequenz* **75**(7–8), 289–300 (2021). <https://doi.org/10.1515/freq-2020-0173>
- Suñé, G. R.: Electron beam lithography for Nanofabrication, pp.1–20 (2008)
- Taghioskoui, M.: Trends in graphene research. *Mater. Today* **12**(10), 34–37 (2009). [https://doi.org/10.1016/S1369-7021\(09\)70274-3](https://doi.org/10.1016/S1369-7021(09)70274-3)
- Tekbryk, K., Ekti, A.R., Kurt, G.K., Görçin, A.: Terahertz band communication systems: challenges, novelties and standardization efforts. *Phys. Commun.* **35**, 100700 (2019). <https://doi.org/10.1016/j.phycom.2019.04.014>
- Varshney, G.: Reconfigurable graphene antenna for THz applications: a mode conversion approach. *Nanotechnology* **31**(13), 135208 (2020a). <https://doi.org/10.1088/1361-6528/ab60cc>
- Varshney, G.: Tunable terahertz dielectric resonator antenna. *Silicon* **13**(6), 1907–1915 (2020b). <https://doi.org/10.1007/s12633-020-00577-0>
- Varshney, G.: Ultra-wideband antenna using graphite disk resonator for THz. *Superlattices Microstruct.* **141**, 106480 (2020c). <https://doi.org/10.1016/j.spmi.2020.106480>
- Varshney, G.: Ultra-wideband antenna using graphite disk resonator for THz applications. *Superlattices Microstruct.* **141**, 106480 (2020h). <https://doi.org/10.1016/j.spmi.2020.106480>
- Varshney, G., Giri, P.: Bipolar charge trapping for absorption enhancement in a graphene-based ultrathin dual-band terahertz biosensor. *Nanoscale Adv.* **3**, 5813–5822 (2021). <https://doi.org/10.1039/d1na00388g>
- Varshney, V.G., Sahana, B.C.: Tunable terahertz circularly polarized dielectric resonator antenna with the higher order modes. *Silicon* **73**, 2021 (2021)
- Varshney, G., Verma, A., Pandey, V.S., Yaduvanshi, R.S., Bala, R.: A proximity coupleld wideband graphene antenna with the generation of higher order TM modes for THz application. *Opt. Mater.* **85**, 456–463 (2018a)
- Varshney, G., Verma, A., Pandey, V.S., Yaduvanshi, R.S., Bala, R.: A proximity coupleld wideband graphene antenna with the generation of higher order TM modes for THz applications. *Opt. Mater.* **85**, 456–463 (2018b)
- Varshney, G., Gotra, S., Pandey, V.S., Yaduvanshi, R.S.: Proximity-coupled two-port multi-input-multi-output graphene antenna with pattern diversity for THz applications. *Nano Commun. Netw.* **21**, 100246 (2019a). <https://doi.org/10.1016/j.nancom.2019.05.003>
- Varshney, G., Gotra, S., Pandey, V.S., Yaduvanshi, R.S.: Proximity-coupled graphene-patch-based tunable single-/dual-band notch filter for THz applications. *J. Electron. Mater.* **48**(8), 4818–4829 (2019b). <https://doi.org/10.1007/s11664-019-07274-8>
- Varshney, G., Debnath, S., Sharma, A.K.: Tunable circularly polarized graphene antenna for THz applications. *Optik* **223**, 165412 (2020). <https://doi.org/10.1016/j.ijleo.2020.165412>
- Wang, X.-C., Zhao, W.-S., Hu, J., Yin, W.-Y.: Reconfigurable terahertz leaky-wave antenna. *IEEE Trans. Nanotechnol.* **14**(1), 62–69 (2015). <https://doi.org/10.1109/TNANO.2014.2365205>
- Wang, R., Ren, X.G., Yan, Z., Jiang, L.J., Sha, W.E.I., Shan, G.C.: Graphene based functional devices: a short review. *Front. Phys.* (2019h). <https://doi.org/10.1007/s11467-018-0859-y>
- Warner, J.H., Schäffel, F., Bachmatiuk, A., Rummeli, M.H.: Applications of graphene, 333–437 (2013)
- Zhang, P., et al.: Application of terahertz spectroscopy and imaging in the diagnosis of prostate cancer. *Curr. Opt. Photonics* **4**(1), 31–43 (2020)

Publisher's Note Springer Nature remains neutral with regard to jurisdictional claims in published maps and institutional affiliations.

Springer Nature or its licensor (e.g. a society or other partner) holds exclusive rights to this article under a publishing agreement with the author(s) or other rightsholder(s); author self-archiving of the accepted manuscript version of this article is solely governed by the terms of such publishing agreement and applicable law.